haematologica
Journal of the Ferrata Storti Foundation

Highly diverse *MECOM* rearrangements uncovered by optical genome mapping and the clinicopathologic features of *MECOM*-rearranged myeloid neoplasms

by Qing Wei, Wei Ying Jen, L. Jeffrey Medeiros, Gokce A. Toruner, Sanam Loghavi, Shimin Hu, Chi Young Ok, Shaoying Li, Jie Xu, Ying S. Zou and Guilin Tang

Received: June 2, 2026.
Accepted: September 16, 2026.

Citation: Qing Wei, Wei Ying Jen, L. Jeffrey Medeiros, Gokce A. Toruner, Sanam Loghavi, Shimin Hu, Chi Young Ok, Shaoying Li, Jie Xu, Ying S. Zou and Guilin Tang. Highly diverse MECOM rearrangements uncovered by optical genome mapping and the clinicopathologic features of MECOM-rearranged myeloid neoplasms.
Haematologica. 2026 Sept 24. doi: 10.3324/haematol.2026.301338 [Epub ahead of print]

Highly diverse *MECOM* rearrangements uncovered by optical genome mapping and the clinicopathologic features of *MECOM*-rearranged myeloid neoplasms

Qing Wei[1], Wei Ying Jen[2], L. Jeffrey Medeiros[1], Gokce A. Toruner[1], Sanam Loghavi[1], Shimin Hu [1], Chi Young Ok [1], Shaoying Li[1], Jie Xu[1], Ying S. Zou[3], Guilin Tang[1]*

[1]Department of Hematopathology, The University of Texas, MD Anderson Cancer Center, Houston, TX, [2]Department of Leukemia, The University of Texas, MD Anderson Cancer Center, Houston, TX, [3]Department of Pathology, Johns Hopkins University School of Medicine, Baltimore, MD

Running Title: *MECOM*-Rearranged Myeloid Neoplasms.

***Corresponding Author**

Guilin Tang, MD, PhD.

Email: gtang@mdanderson.org

Department of Hematopathology, The University of Texas, MD Anderson Cancer Center

6565 MD Anderson Blvd, Houston, Texas 77030-4009

Authorship Contributions

Conceptualization and study design: GT; data curation and analysis: QW, WYJ, GT, LJM, SH, GAT, SL, CO, SLi, and JX; manuscript drafting: QW, GT, and LJM; manuscript review and editing: All authors.

Data-sharing statement

All relevant clinical, cytogenetic, and molecular data included in this study are available from the corresponding author upon reasonable request, subject to institutional and ethical regulations governing patient data protection.

Conflicts of Interest:

The authors declare no conflict of interests.

Fundings:

No funding for this study.

MECOM rearrangements (*MECOM*-R) occur in a spectrum of myeloid neoplasms and are recognized as a class-defining genetic abnormality associated with adverse prognosis in current classification and risk stratification systems.[1-3] The classic inv(3)/t(3;3)(q21.3;q26.2) leads to *GATA2::MECOM* through enhancer hijacking. However, more than half of *MECOM*-R cases have diverse variant partner loci and exhibit considerable structural heterogeneity.[4-6] Detection of *MECOM*-R remains challenging because a subset of rearrangements is cryptic by conventional cytogenetics and many do not generate fusion transcripts detectable by RNA sequencing (RNAseq). Optical genome mapping (OGM) is a genome-wide cytogenomic platform capable of detecting structural variants at high resolution and has shown promise in identifying cryptic *MECOM*-R.[7-9] In this study, we analyzed a cohort of 330 patients with *MECOM*-rearranged myeloid neoplasms to characterize their clinicopathologic and molecular features. Among these, 101 patients underwent OGM and allowing for detailed cytogenomic analysis, including characterization of the breakpoint landscape, structural diversity of *MECOM*-R, and comparison of OGM with chromosomal analysis, fluorescence in situ hybridization (FISH), and RNAseq for *MECOM*-R detection. This study was approved by the Institutional Review Board and was conducted in accordance with the Declaration of Helsinki.

MECOM-R was confirmed by FISH using *MECOM* break-apart probes and/or OGM in all cases. For OGM cases, putative partner genes were assigned according to the genomic breakpoint: for intragenic breakpoints, the disrupted gene was designated as the putative partner gene; for intergenic breakpoints, the putative partner gene was assigned as the nearest annotated gene to the breakpoint, or when applicable, a nearby recurrently reported *MECOM* partner gene. For

cases without OGM, putative partner genes were assigned based on previously reported *MECOM* partner genes involving corresponding chromosomal bands.

This study included 330 patients with myeloid neoplasms harboring *MECOM*-R, 185 females and 145 males, with a median age of 65 years (range, 2–92). The diagnoses included acute myeloid leukemia (80%), blast phase of myeloproliferative neoplasm (11%), myelodysplastic syndrome (8%), and other entities (1%). *MECOM*-R was detected at initial diagnosis in 62% of cases and acquired during disease progression and/or relapse in 38% of cases. The classic *GATA2*::*MECOM* was identified in 47% of cases, variant *MECOM*-R in 50% of cases, and unknown in 3% of cases. In cases with variant *MECOM*-R, 42 partner loci /genes were identified involving chromosomes 1–8, 10–13, 17, and 21 (**Figure 1A**).

Among the 101 cases analyzed by OGM, 63% showed variant *MECOM*-R, a significantly higher proportion than that observed in the 229 cases evaluated by only conventional karyotyping and FISH (63% vs. 44%, $p < 0.001$) **(Table 1)**.

Putative partner genes/loci are summarized in **Table 1**. Among the 42 variants *MECOM*-R identified in the whole cohort, 8 were detected in ≥ 5 cases, 11 in 2~3 cases and 23 partner loci were identified in single cases. In addition to the classic partner locus 3q21/*GATA2,* 13 additional partner loci were identified on chromosome 3 in 38 (11.5%) cases, with 3p23-p25 being most frequent (6% of total cases) **(Figure 1B).**

Among the 101 cases analyzed by OGM, 76 harbored *MECOM*-R as the only clinically significant rearrangement. The remaining 25 cases showed additional rearrangements, including chromoanagenesis in 17 cases, t(9;22)/*BCR::ABL1* in 5 cases (all chronic myeloid leukemia), and one case each of inv(16)(p13.3q24.3)/*CBFA2T3::GLIS2*, (4;21)(q12;q22.12) /*RUNX1::AP000331.1*, and t(5;21)(q31.3;q22.12)/*RUNX1::ARHGAP26*.

Among the 101 cases analyzed by OGM, breakpoints at the 3q26.2 locus were located within *MECOM* in 69 and outside of *MECOM* in 32 cases. Among cases with intragenic *MECOM* breakpoints, most occurred in introns 1 or 2 (76%). For the cases with breakpoints outside of *MECOM*, 21 were centromeric and 11 telomeric to *MECOM* **(Figure 1C).**

Breakpoint distribution at 3q26.2 showed distinct patterns according to partner genes. Rearrangements involving *SATB1*, *MYC*, *ARID1B,* and *MYB* had breakpoints exclusively or predominantly within intron 1 or 2 of *MECOM*. In contrast, *ETV6*, *NRIP1*, and *MBNL1* were more commonly associated with breakpoints in other *MECOM* introns. *CDK6*-associated breakpoints were predominantly centromeric to *MECOM* (4 of 5 cases) and *THADA*-associated breakpoints were mainly telomeric (3 of 4 cases). *MECOM* breakpoint location correlated with RNAseq results. Breakpoints within introns 1 or 2, or in adjacent extragenic regions were not associated with detectable fusion transcripts, consistent with an enhancer hijacking mechanism. In contrast, breakpoints located within other *MECOM* introns generated in-frame fusion transcripts.

The sensitivity of different assays for detecting *MECOM*-R is summarized in **Supplemental Table 1**. Among the 101 cases evaluated by OGM, karyotyping detected 3q26.2 rearrangements in only 61% cases. The common cryptic chromosomal rearrangements involving *MECOM* included t(3;7)(q26.2;q21.2) (4/5 cases, all 5 cases exhibited unbalanced translocations or highly complex rearrangements/chromoanagenesis involving chromosome 3) and variants inv(3) (13/18 cases) **(Figure 2A)**. FISH demonstrated high sensitivity, detecting *MECOM*-R in 75 of 79 (95%) cases. Four cases with *MECOM*-R were undetected by FISH: 3 due to small insertions (**Figure 2B-2C**) and 1 due to complex rearrangements involving the 3q26.2 locus. Among the 74 cases with concurrent RNAseq, only 14 (19%) showed fusion transcripts, with fusion genes of *RPN1, RUNX1*, *MBNL1*, *NRIP1*, *ETV6*, and *HNRNPD*. Among *GATA2::MECOM* cases, 3/30 showed *RPN1::MECOM* fusion transcripts. Among three cases with *ETV6::MECOM*, one showed fusion transcripts, indicating different mechanisms involved in *MECOM* activation.

Clinicopathologic, cytogenetic, and molecular features associated with *MECOM*-R are summarized in **Supplemental Figure 1**. Megakaryocytic dysplasia was observed in 74% of cases in the entire cohort: 77% of cases with classic *MECOM*-R and 50% to 92% of cases in variant groups. Dysplastic megakaryocytic hyperplasia was present in 19% of classic *MECOM*-R cases, compared with 0-17% across variant *MECOM*-R groups.

Complex karyotypes and del(7q)/-7 were identified in 40% and 53% of cases, respectively. No significant differences in the frequencies of complex karyotype or del(7q)/-7 were observed between classic and variant *MECOM*-R groups.

Among 234 cases with molecular mutation data, *RTK/RAS* pathway (*CBL, FLT3, GNAS, JAK1, JAK2, JAK3, KIT, KRAS, MAP2K1, MPL, NRAS, PTPN11*) mutations were most frequent (58%), followed by *TP53* (20%) and *SF3B1* (20%). *RTK/RAS* mutations were significantly less frequent in *MYC::MECOM* cases (40% vs 69% in *GATA2::MECOM*, p=0.04). *SF3B1* mutations were significantly less frequent in cases with *RUNX1::MECOM* (7%) or *SATB1::MECOM* (5%), compared with 30% in *GATA2::MECOM* (p=0.02).

Overall survival was analyzed among patient subgroups with 10 or more cases **(Supplemental Figure 2)**. There was no significant difference in overall survival among six *MECOM*-R subgroups (p = 0.62). Median overall survival was 16 months for patients with *GATA2::MECOM*, 11 months for *RUNX1::MECOM*, 16 months for *ETV6::MECOM*, 15 months for *SATB1::MECOM*, 13 months for *MYC::MECOM*, and 13 months for *THADA::MECOM*.

This study represents the largest analysis of *MECOM*-rearranged myeloid neoplasms to date and provides an integrated cytogenetic, molecular, and clinicopathologic characterization of this entity. By incorporating OGM, we demonstrate that *MECOM*-R with variant partners account for more than 60% of cases, involving a broad spectrum of loci across multiple chromosomes, and approximately one-third of cases were cryptic by karyotyping. This cohort also expands the landscape by identifying several rarely reported partners, including *MBNL1, IL12A-AS1*, *FNDC3B* and *G3BP1,* and previously underrecognized partners such as *MYB, ANGPT1, GRM7,* and *HNRNPD*. OGM further revealed that most breakpoints involving intron 1 or 2 of *MECOM* or adjacent extragenic regions were not associated with detectable fusion transcripts, supporting

enhancer hijacking as a major mechanism of *MECOM* activation, and providing a mechanistic explanation for the limited sensitivity of RNAseq in detecting *MECOM*-R.[8,10,11]

Our findings also demonstrated that OGM substantially improves the detection and characterization of cryptic and variant *MECOM*-R compared with conventional cytogenetics, FISH and RNAseq. As OGM becomes more widely adopted in clinical laboratories, it has the potential to serve as a first-line genomic assay for myeloid neoplasms, lymphoid neoplasms (such as B-/T-ALL), mixed-phenotype acute leukemia, and myeloma. In centers where OGM is unavailable, *MECOM* FISH should be considered in cases with -7/del(7q), *SF3B1* mutations, or clinicopathologic features suggestive of *MECOM*-R despite the absence of a detectable 3q26.2 abnormality by chromosome analysis.

Despite marked genetic heterogeneity, variant *MECOM*-R subgroups largely shared the clinicopathologic features of classic *GATA2::MECOM*, including frequent megakaryocytic dysplasia, del(7q)/-7, and *SF3B1* and *RTK/RAS* pathway mutations.[12,13] Although selected differences in morphologic and mutational profiles were observed among subgroups, these differences did not translate into overall survival.[14] These findings suggest that structurally diverse *MECOM*-R converge on a common pathogenic mechanism and support the current classification that recognize all *MECOM*-rearranged neoplasms as a unified high-risk entity.[1,2,15]

We acknowledge that this study has limitations. 1) Although OGM accurately defines genomic breakpoint locations, it cannot determine whether the putative partner genes drive *MECOM* activation; 2) For cases without OGM or sequencing confirmation, partner gene assignments

based on cytogenetic breakpoint locations remain presumptive because conventional cytogenetics lacks gene-level resolution; 3) Quantitative MECOM expression was not evaluated. Future studies integrating transcriptomic profiling would likely further clarify the mechanisms of *MECOM* activation and the biological significance of different partner loci.

In summary, OGM significantly improves detection and structural characterization of *MECOM*-R and reveals a high frequency of cryptic and variant events. While variant partner genes contribute to genomic diversity and selected clinicopathologic differences, they do not appear to affect prognosis, supporting the current classification systems that group all *MECOM*-rearranged neoplasms into a single high-risk category, regardless of the underlying fusion partner.

References

1. Arber DA, Orazi A, Hasserjian RP, et al. International Consensus Classification of Myeloid Neoplasms and Acute Leukemias: integrating morphologic, clinical, and genomic data. Blood. 2022;140(11):1200-1228.
2. Khoury JD, Solary E, Abla O, et al. The 5th edition of the World Health Organization Classification of Haematolymphoid Tumours: myeloid and histiocytic/dendritic neoplasms. Leukemia. 2022;36(7):1703-1719.
3. Dohner H, Wei AH, Appelbaum FR, et al. Diagnosis and management of AML in adults: 2022 recommendations from an international expert panel on behalf of the ELN. Blood. 2022;140(12):1345-1377.
4. Tang Z, Tang G, Hu S, et al. Deciphering the complexities of MECOM rearrangement-driven chromosomal aberrations. Cancer Genet. 2019;233-234:21-31.
5. Ottema S, Mulet-Lazaro R, Beverloo HB, et al. Atypical 3q26/MECOM rearrangements genocopy inv(3)/t(3;3) in acute myeloid leukemia. Blood. 2020;136(2):224-234.
6. Gao J, Gurbuxani S, Zak T, et al. Comparison of myeloid neoplasms with nonclassic 3q26.2/MECOM versus classic inv(3)/t(3;3) rearrangements reveals diverse clinicopathologic features, genetic profiles, and molecular mechanisms of MECOM activation. Genes Chromosomes Cancer. 2022;61(2):71-80.
7. Levy B, Baughn LB, Akkari Y, et al. Optical genome mapping in acute myeloid leukemia: a multicenter evaluation. Blood Adv. 2023;7(7):1297-1307.
8. Ok CY, Tang G, Loghavi S, et al. Comparative analysis of targeted RNA-seq and optical genome mapping for detecting gene rearrangements in acute leukemia. Cancers (Basel). 2025;17(21):3458.
9. Tang G, Wei Q, Klausner M, Zou YS, Toruner GA. Optical genome mapping in myeloid neoplasms. Hum Pathol. 2026:106176.
10. Groschel S, Sanders MA, Hoogenboezem R, et al. A single oncogenic enhancer rearrangement causes concomitant EVI1 and GATA2 deregulation in leukemia. Cell. 2014;157(2):369-381.
11. Ottema S, Mulet-Lazaro R, Erpelinck-Verschueren C, et al. The leukemic oncogene EVI1 hijacks a MYC super-enhancer by CTCF-facilitated loops. Nat Commun. 2021;12(1):5679.
12. Groschel S, Sanders MA, Hoogenboezem R, et al. Mutational spectrum of myeloid malignancies with inv(3)/t(3;3) reveals a predominant involvement of RAS/RTK signaling pathways. Blood. 2015;125(1):133-139.
13. Huber S, Haferlach T, Meggendorfer M, et al. SF3B1 mutations in AML are strongly associated with MECOM rearrangements and may be indicative of an MDS pre-phase. Leukemia. 2022;36(12):2927-2930.

14. Jen WY, Tang G, Kugler E, et al. MECOM fusion partner and bone marrow blast percentage influence outcomes of patients with MECOM rearranged acute myeloid leukaemia. Br J Haematol. 2025;207(6):2451-2461.
15. Joshi U, Shallis RM. MECOM-Rearranged Acute Myeloid Leukemia: pathobiology and management strategies. Hematol Rep. 2025;17(6):59.

Table 1: Partner loci/putative partner genes identified by optical genome mapping (OGM) (n=101) or by karyotyping and FISH (n=229).

Partner Loci/ putative genes*	**Total cohort**	**With OGM**	**Without OGM**	Continues		
3q21.3/*GATA2*	156	37	119	**Partner Loci/genes**	**Total cohort**	**Without OGM**
21q22/*RUNX1*	32	6	26	3p23-p25**	15	15
12p13/*ETV6*	21	5	16	3p13	2	2
8q24.2/*MYC*	15	5	10	11q23	2	2
2p21/*THADA*	12	4	8	1p22	1	1
6q25.3/*ARID1B*	6	3	3	2q21	1	1
17q22 /*MSI2*	6	1	5	3q12	1	1
3p24.3/*SATB1*	5	5	0	4p14	1	1
7q21.2/*CDK6*	5	5	0	5q33/*G3BP1*	1	1
3q25.1/*MBNL1*	3	3	0	10q22	1	1
21q11.2/*NRIP1*	3	3	0	12q21	1	1
3p26.1/*GRM7* #	2	2	0	12q22	1	1
3q25.33/*IL12A-AS1*	2	2	0	13q12	1	1
6q23.2/*MYB* #	2	2	0	17q25	1	1
8q23.1/*ANGPT1* #	2	2	0	Unknown***	10	10
4q21.22/*HNRNPD* #	2	1	1			
3q24/*CPB1* #	2	1	1			
3q27.2/*TRA2B*	2	1	1			
1q42.3/*IRF2BP2* #	1	1	0			
2p16.1/*BCL11A*	1	1	0			
2q22.3/*ARHGAP15* #	1	1	0			
3q25.2/*P2RY1* #	1	1	0			
3q26.31/*FNDC3B*	1	1	0			
3q26.33/*FXR1* #	1	1	0			
3q29/ *TMEM207* #	1	1	0			
4q32.1/ *RAPGEF2* #	1	1	0			
5q13.1/*PIK3R1* #	1	1	0			
5q13.3/*F2R* #	1	1	0			
6p25.2/*TUBB2A* #	1	1	0			
13q14.13/*GTF2F2* #	1	1	0			
13q31.3/*LINC0037* #	1	1	0			
Total	330	101	229			

*Putative partner gene designation. For cases analyzed by OGM, putative partner genes were assigned based on intragenic breakpoints or genomic proximity to the breakpoint. For cases without OGM, putative partner genes were assigned based on previously reported recurrent *MECOM* partner genes or chromosomal bands corresponding to partner genes identified by OGM. These putative partner genes represent positional candidate genes based on genomic proximity and are not necessarily functional fusion partners.

**3p23-p25 band designation was based on the *MECOM* FISH map-back analysis on G-banded metaphase chromosomes. ****MECOM*-R was detected by FISH, whereas karyotyping showed either unidentified material at 3q26.2 or a normal chromosome 3. # novel loci/putative partner genes.

Figure Legends

Figure 1. Distribution of *MECOM* rearrangement (*MECOM*-R) partner loci and the breakpoints locations at 3q26.2. **A.** Circos plot illustrates the distribution of *MECOM*-R partner loci in the entire cohort excepting 10 unknown cases (n=320). A total of 43 loci across 14 chromosomes are identified. The 1-22, X and Y indicate the chromosome number. Arcs represent rearrangements linking 3q26.2 (*MECOM*) to partner loci. **B**. Distribution and frequency of chromosome 3 partner loci involved in inv(3)/t(3;3) associated *MECOM*-R . **C**. Breakpoints distribution at the 3q26.2 locus identified optical genome mapping (n=101). Breakpoints are categorized as intragenic (orange) and extragenic (green, centromeric; blue, telomeric). The top panel depicts genomic coordinates, exon–intron layout, and orientation of the *MECOM* gene.

Figure 2. Detection of *MECOM* rearrangements by optical genome mapping (OGM), karyotyping and FISH (n=101). **A**. Sankey diagram showing the distribution of partner loci/genes (including the case number in each subgroup) identified by OGM. Green flows indicate rearrangements detected by concurrent karyotyping (total 62 cases), while red flows indicate rearrangements missed by karyotyping (total 39 cases). Flow width corresponds to the number of cases. **B-C**. A representative case of ins(3;12) resulting in *ETV6::MECOM*, cryptic by karyotyping and FISH. **B**. Circos plot demonstrates the rearrangement consistent with t(3;12) or ins(3;12). **C**. Genome browser view showing insertion of *ETV6* into *MECOM* at intron 2, generating the *ETV6::MECOM* fusion (middle blue bar).

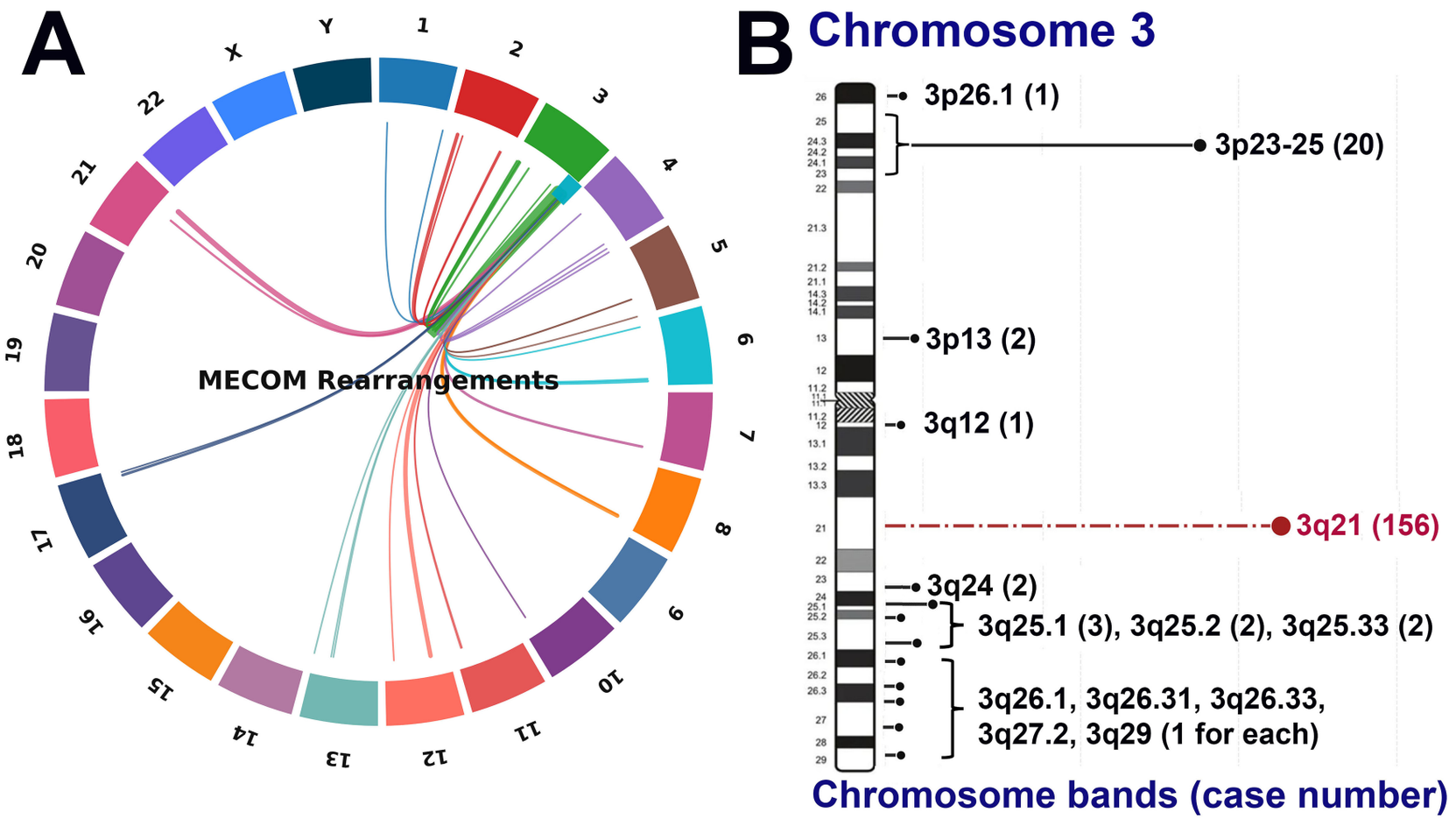
A
MECOM Rearrangements
B Chromosome 3
3p26.1 (1)
3p23-25 (20)
3p13 (2)
3q12 (1)
3q21 (156)
3q24 (2)
3q25.1 (3), 3q25.2 (2), 3q25.33 (2)
3q26.1, 3q26.31, 3q26.33,
3q27.2, 3q29 (1 for each)
Chromosome bands (case number)

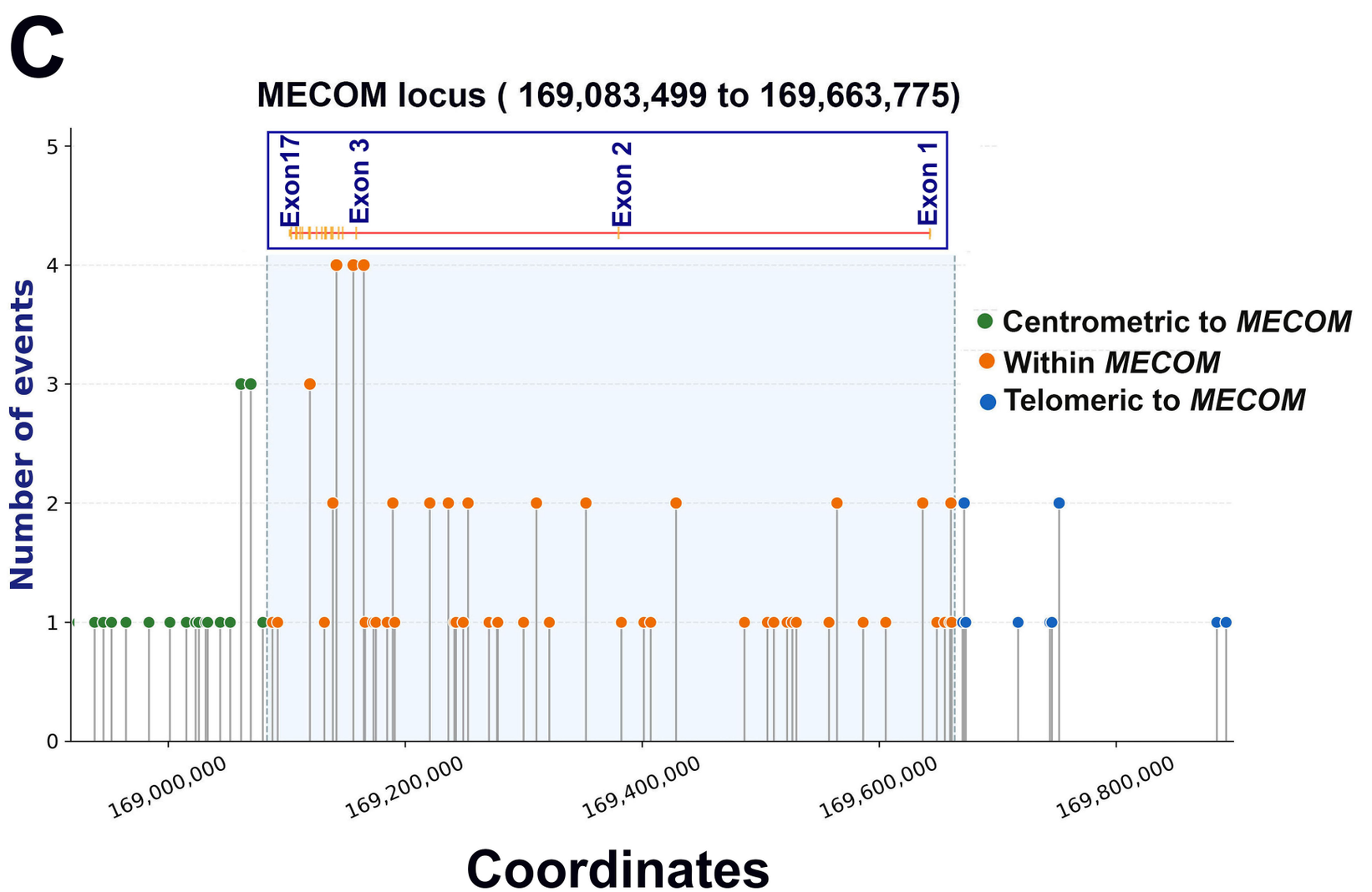
C
MECOM locus (169,083,499 to 169,663,775)
Exon17
Exon 3
Exon 2
Exon 1
Number of events
Centrometric to MECOM
Within MECOM
Telomeric to MECOM
169,000,000
169,200,000
169,400,000
169,600,000
169,800,000
Coordinates

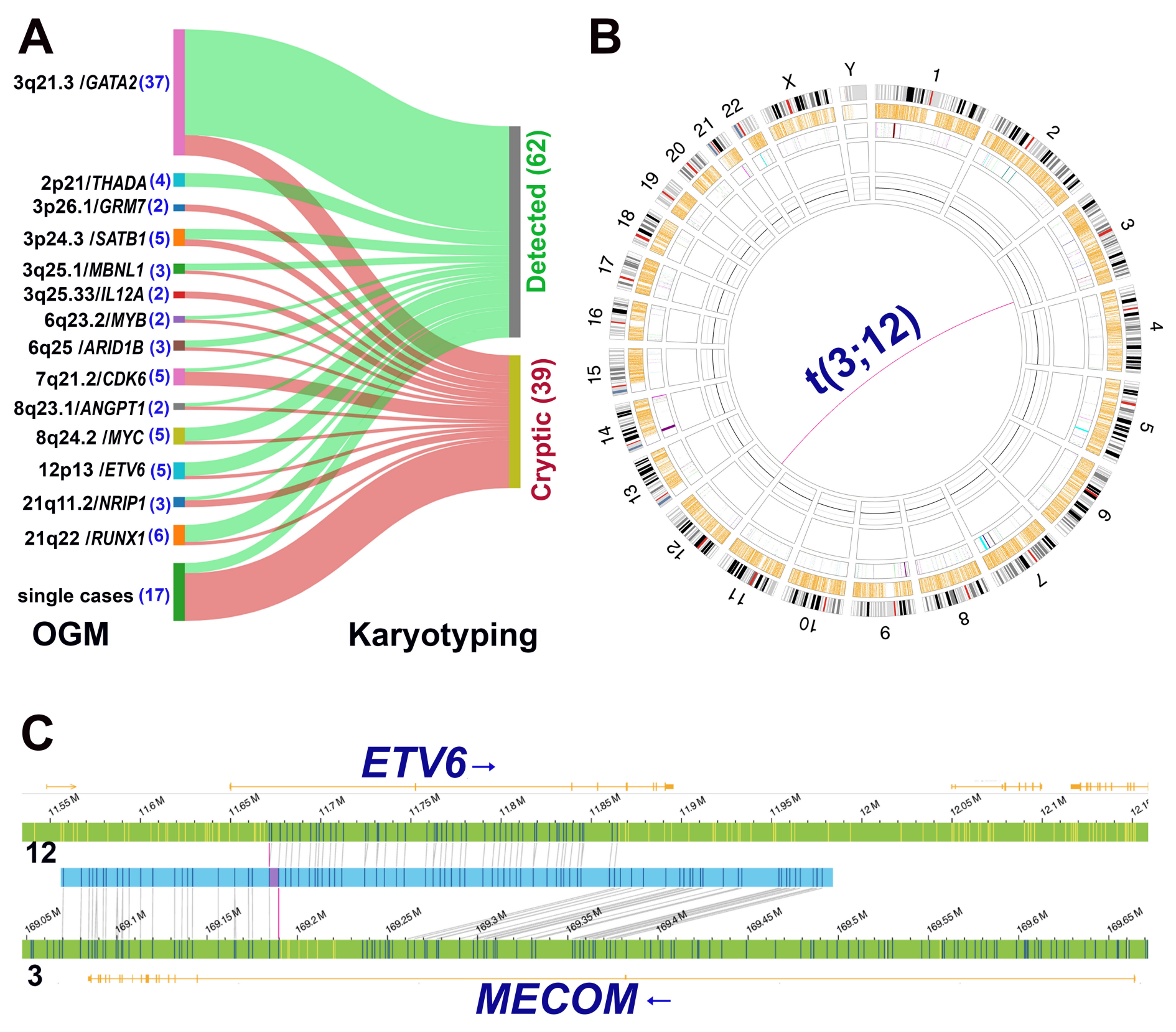
A
3q21.3 /GATA2 (37)
2p21/THADA (4)
3p26.1/GRM7 (2)
3p24.3 /SATB1 (5)
3q25.1/MBNL1 (3)
3q25.33/IL12A (2)
6q23.2/MYB (2)
6q25 /ARID1B (3)
7q21.2/CDK6 (5)
8q23.1/ANGPT1 (2)
8q24.2 /MYC (5)
12p13 /ETV6 (5)
21q11.2/NRIP1 (3)
21q22 /RUNX1 (6)
single cases (17)
Detected (62)
Cryptic (39)
OGM
Karyotyping
B
t(3;12)
C
ETV6→
12
3
←MECOM

Supplemental Table 1. Detection rates of *MECOM* rearrangements (-R) by karyotyping, FISH, and RNA fusion assay in 101 cases with *MECOM*-R identified by optical genome mapping, stratified by partner chromosomal loci/genes.

Partner Loci/genes	OGM	Detected by karyotyping	FISH		RNA sequencing	
			Performed	Positive	Performed	Positive
3q21.3 /*GATA2*	37	31	**31**	**29**	30	3
21q22 /*RUNX1*	6	5	5	5	3	3
3p24.3 /*SATB1*	5	3	4	4	3	0
8q24.2 /*MYC*	5	4	3	3	4	0
12p13 /*ETV6*	5	4	**4**	**3**	3	1
7q21.2/*CDK6*	5	1	3	3	3	0
2p21 /*THADA*	4	4	3	3	2	0
3q25.1/*MBNL1*	3	2	2	2	3	3
6q25 /*ARID1B*	3	2	2	2	2	0
21q11.2/*NRIP1*	3	1	3	3	3	3
3p26.1/*GRM7*	2	0	1	1	2	0
3q25.33/*IL12A-AS1*	2	0	2	2	2	0
6q23.2/*MYB*	2	1	1	1	1	0
8q23.1/*ANGPT1*	2	1	0	0	1	0
1q42.3/ *IRF2BP2*	1	0	1	1	1	0
2p16.1/*BCL11A*	1	1	1	1	1	0
2q22.3/*ARHGAP15*	1	0	1	1	0	NA
3q24/*CPB1*	1	0	1	1	1	0
3q25.2/*P2RY1*	1	0	0	0	1	0
3q26.31/*FNDC3B*	1	0	1	1	1	0
3q26.33/*FXR1*	1	0	1	1	1	0
3q27.2/*TRA2B*	1	0	1	1	0	NA
3q29/*TMEM207*	1	0	1	1	1	0
4q21.22/*HNRNPD*	1	1	1	1	1	1
4q32.1/*RAPGEF2*	1	0	1	1	0	NA
5q13.1/*PIK3R1*	1	0	1	1	1	0
5q13.3/*F2R*	1	0	**1**	**0**	1	0
6p25.2/*TUBB2A*	1	0	1	1	0	NA
13q14.13/*GTF2F2*	1	0	1	1	1	0
13q31.3/*LINC0037*	1	0	1	1	1	0
17q22 /*MSI2*	1	1	0	0	0	0
Total (sensitivity %)	101	**62 (61%)**	79	**75 (95%)**	74	**14 (19%)**

Supplemental Figure 1

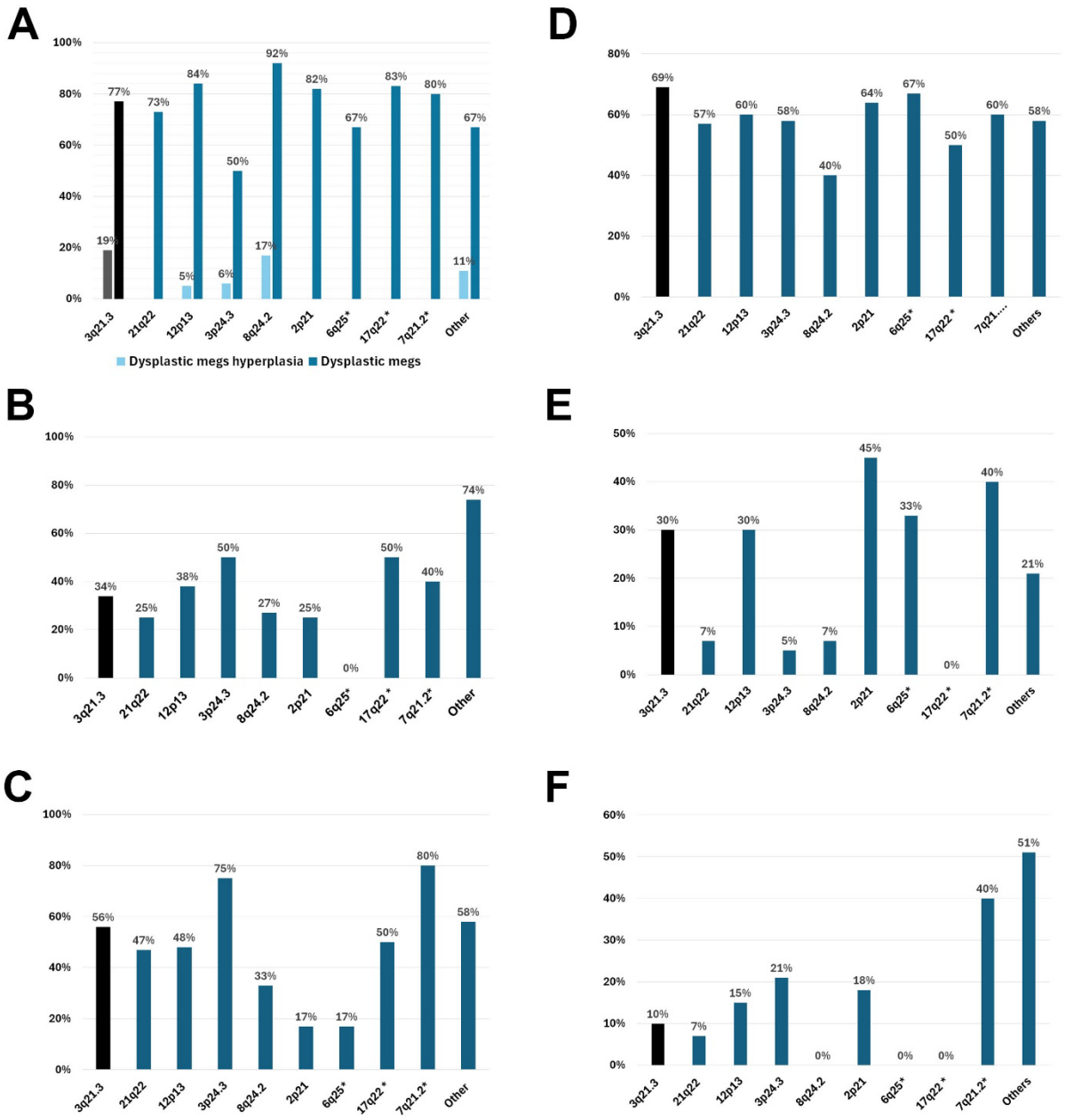

Supplemental Figure 1: Clinicopathologic and molecular features across common (n≥5) *MECOM*-R subgroups.
A. Frequency of megakaryocytic dysplasia and dysplastic megakaryocytic hyperplasia.
B. Frequency of complex karyotype.
C. Frequency of monosomy 7 and/or del(7q).
D. Frequency of *RTK/RAS* pathway mutations.
E. Frequency of *SF3B1* mutations.
F. Frequency of *TP53* mutations.
The classic *GATA2::MECOM* group (3q21.3) is shown in black, and variant subgroups are shown in blue.
Percentages represent the proportion of cases within each subgroup harboring the indicated feature.
Asterisks (*) denote subgroups with fewer than 10 cases.
3p24.3 subgroup: comprises cases with 3p24.3 identified by OGM, and cases with 3p23-p25 by karyotyping

Supplemental Figure 2.

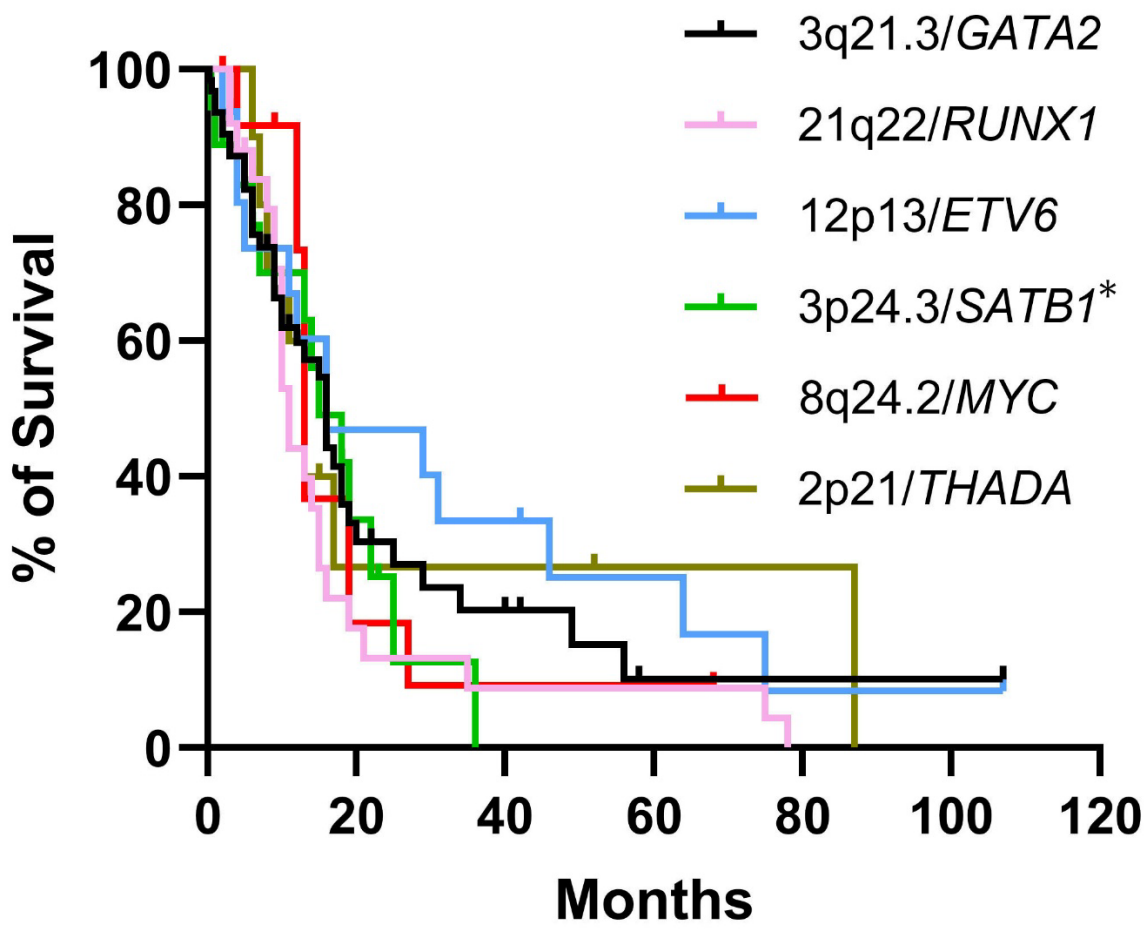

Supplemental Figure 2: Overall survival across MECOM rearrangement subgroups. Kaplan-Meier analysis demonstrating no statistically significant different in overall survial among the six subgroups with >= 10 cases

*Comprises cases with 3p24.3 identified by OGM and cases with 3p23-p25 by karyotyping